Direct kinetic parameter estimation from dynamic ECT sinogram using dimension-reduced time-activity basis [1]

JS Maltz†‡, *Member, IEEE*; BW Reutter†, *Member, IEEE*;
RH Huesman†, *Senior Member, IEEE*; and TF Budinger†‡, *Member, IEEE*
†Center for Functional Imaging, Lawrence Berkeley National Laboratory
‡Department of Electrical Engineering and Computer Science, University of California at Berkeley

Abstract

We present an algorithm of reduced computational cost which is able to estimate kinetic model parameters directly from dynamic ECT sinograms. The algorithm exploits the extreme degree of parameter redundancy inherent in linear combinations of the exponential functions which represent the modes of first order compartmental systems. The singular value decomposition is employed to find a small set of orthogonal functions, the linear combinations of which are able to accurately represent all modes within the physiologically anticipated range in a given study. The reduced-dimension basis is formed as the convolution of this orthogonal set with a measured input function. The Moore-Penrose pseudoinverse is used to find coefficients of this basis. Algorithm performance is evaluated at realistic count rates using MCAT phantom and clinical ^{99}Tc-teboroxime myocardial study data. Recovered tissue responses compare favorably with those obtained using more computationally intensive methods.

I. Introduction

Most contemporary techniques for the reconstruction of emission computed tomography (ECT) images assume that the projection data are obtained from a radionuclide source distribution which does not vary in time. In most functional studies which involve the use of a rotating camera which cannot acquire projections over 360° simultaneously, this is a poor assumption. There exists, consequently, a need for algorithms capable of solving the dynamic ECT reconstruction problem, which involves the estimation not only of the underlying functional anatomic source geometry, but also of the pharmacokinetics of injected radiotracer materials.

Reutter et al. have demonstrated an algorithm capable of fitting single compartment models directly to the projections of both phantom and clinical myocardial studies [1, 2]. A stabilized Newton-Raphson optimization algorithm is used to solve the non-linear weighted least squares problem whose solution yields the kinetic parameters directly from the acquired projection data. While this method is effective in providing the desired estimates, the amount of computation required is large for studies involving many dynamic regions. The objective of the approach presented here is to reduce these requirements through dimensionality reduction and linearization of the problem.

[1]This work was supported by US Department of Health and Human Services grants HL-07367, R01-HL50663 and P01-HL25840, by US Department of Energy contract DE-AC03-76SF00098 and by the South African National Research Foundation.

Linear algorithms for the estimation of the kinetic parameters in dynamic ECT, which employ a preselected time-activity basis of exponential functions, have been presented in the past [3, 4]. Preselection of the kinetic basis converts a problem which is non-linear in the exponential rate parameters into a much simpler linear problem. Basis sets used by these algorithms are typically composed of families of decaying real exponential functions having rate constants selected so as to span the range of physiologically feasible modes expected in the data. For example, Cunningham et al. utilized a set of $M = 100$ sampled exponential functions:

$$f_{\tilde{m}}[l] = \mathrm{e}^{-k_{\tilde{m}}\, l\, \Delta t}, \qquad l = 0, 1, 2, \ldots, L-1, \tag{1}$$

where l is a discrete time index and $k_{\tilde{m}} \in [10^{-4},\ 1]$ s^{-1}. The $k_{\tilde{m}}$ were spaced logarithmically on this interval, whose bounds were selected for the application of exponential spectral analysis to cerebral positron emission tomography (PET) studies using three different tracer agents.

As we have shown previously, an orthogonal basis set of 6 functions (sampled regularly at 32 points in $t \in [0,\, 300\, s]$), is able to approximate any one of these $f_{\tilde{m}}$ with a maximum deviation of well under 1% [5]. The large dimensionality reduction possible illustrates the well-known high level of redundancy that exists among families of closely parameterized real decaying exponentials [6, 7]. Here, we exploit this redundancy to achieve significant computational savings over previous algorithms for exponential spectral analysis.

II. Problem formulation

We begin by assuming that the underlying source distribution $\Omega(\mathbf{x})$ has been segmented into several regions of interest (ROI's) $\Omega_n(\mathbf{x}),\ n = 1, 2, \ldots, N$.

For the application of the algorithm to myocardial studies during which both wash-in and wash-out of the tracer occur, such as those involving ^{99}Tc-teboroxime, we assume that tracer kinetics are governed by a single compartment model. To cope with possible region heterogeneity [8], we incorporate additional flexibility in allowing the time-activity curve (TAC) of each ROI to be composed of linear combinations of the responses of several such models:

$$I_n(t) = \sum_{\tilde{m}=1}^{\tilde{M}} k_{21}^{\tilde{m}n}\, i(t) * \mathrm{e}^{-k_{12}^{\tilde{m}} t}, \tag{2}$$

where $i(t)$ is the measured blood input function, and the '$*$' operator denotes convolution.

As in [5], we form the $(L \times \tilde{M})$ matrix $\mathbf{X}$ whose $\tilde{m}$th column is $f_{\tilde{m}}[l]$ as defined in (1), and invoke the singular value decomposition (SVD) to find orthogonal basis vectors for the range of $\mathbf{X}$. These are the left singular (column) vectors $\mathbf{u}_{\tilde{m}}$ of the SVD of $\mathbf{X}$:

$$\mathbf{X} = \mathbf{V}\mathbf{S}\tilde{\mathbf{U}}^T, \qquad \tilde{\mathbf{U}} = \left(\mathbf{u}_1\ \mathbf{u}_2\ \cdots\ \mathbf{u}_{\tilde{M}}\right) \tag{3}$$

where $\mathbf{V}$ is the matrix of right singular vectors, and $\mathbf{S}$ is the diagonal matrix of singular values. We associate the discrete time index l with each row of $\mathbf{U}$. Depending on the degree of accuracy required in the sampled representation of the $I_n(t)$, we utilize only the first $M \leq \tilde{M}$ of $\tilde{\mathbf{U}}$ such that:

$$\mathbf{U} = \left(\mathbf{u}_1\ \mathbf{u}_2\ \cdots\ \mathbf{u}_M\right). \tag{4}$$

Typically, $M \approx 4$ is sufficient for the myocardial imaging applications we have studied.

We then form the matrix $\mathbf{C}$ from the columns of $\mathbf{U}$ convolved with the sampled blood input function $i[l]$, which we assume has either been measured or estimated:

$$\mathbf{C}' = \left(\mathbf{c}_1\ \mathbf{c}_2\ \cdots\ \mathbf{c}_M\right). \tag{5}$$

where $\mathbf{c}_m = \mathbf{u}_m * i[l],\ l = 0, 1, \ldots, L-1$.

With the kinetic model formalized, we wish to estimate the coefficients μ_{mn} of the $\mathbf{c}_m$ for all regions, which form the approximated TAC's as:

$$\hat{I}_n[l] = \sum_{m=1}^{M} \hat{\mu}_{mn}\, \mathbf{c}_m[l], \qquad l = 0, 1, \ldots, L-1\,; \tag{6}$$

where $L = RP$, the total number of angular projections, given R camera rotations with P angular projections per rotation, and Q bins per projection.

III. Problem Solution

We begin by lexicographically stacking the projections of the $RP \times Q$ measured sinogram $\tilde{\mathbf{Y}}$ into the vector $\tilde{\mathbf{y}}$. Similarly the $P \times Q$ sinogram $\mathbf{Y}'_n$ for each of the N segmented regions $f_n(\mathbf{x})$ are stacked into the vectors $\mathbf{y}'_n$. We then define the $RPQ \times M$ matrices $\mathbf{G}_n$ which consist of $R \times M$ replicates of $\mathbf{y}'_\mathbf{n}$. The geometric weighting matrix for the activity contributions of each region is then given by:

$$\mathbf{G} = \left[\ \mathbf{G}_1 \quad \mathbf{G}_2 \quad \cdots \quad \mathbf{G}_N\ \right]. \tag{7}$$

The second matrix we will describe consists of blocks containing the convolved basis functions $\mathbf{c}_m$. For each time sample l, we form the $PQ \times M$ matrices

$$\mathbf{C}_l = \begin{bmatrix} u_1[l] & u_2[l] & \cdots & u_M[l] \\ u_1[l] & u_2[l] & \cdots & u_M[l] \\ \vdots & \vdots & \vdots & \vdots \\ u_1[l] & u_2[l] & \cdots & u_M[l] \end{bmatrix} \tag{8}$$

from which the $RPQ \times NM$ basis weighting matrix

$$\mathbf{C} = \begin{bmatrix} \mathbf{C}_0 & \mathbf{C}_0 & \cdots & \mathbf{C}_0 \\ \mathbf{C}_1 & \mathbf{C}_1 & \cdots & \mathbf{C}_1 \\ \vdots & \vdots & \vdots & \vdots \\ \mathbf{C}_{L-1} & \mathbf{C}_{L-1} & \cdots & \mathbf{C}_{L-1} \end{bmatrix} \tag{9}$$

is composed.

The vector $\hat{\boldsymbol{\mu}}$ containing the coefficient estimates μ_{mn} is easily obtained via solution of the linear system:

$$\tilde{\mathbf{y}} = \mathbf{F}\,\hat{\boldsymbol{\mu}} = (\mathbf{G} \cdot \mathbf{C})\,\hat{\boldsymbol{\mu}} \tag{10}$$

where the operator '$\cdot$' denotes element-by-element multiplication.

Equation 10 may then be solved by the method of least squares for the kinetic parameters

$$\hat{\boldsymbol{\mu}} = (\mathbf{F}^T\mathbf{F})^{-1}\mathbf{F}^T\tilde{\mathbf{y}}, \tag{11}$$

when $(\mathbf{F}^T\mathbf{F})$ is invertible. When this is not the case, the SVD may be used to find the pseudoinverse. This is unlikely, since (10) is typically highly overdetermined, owing to the fact that the number of projection measurements acquired in a typical ECT study far exceed the number of parameters to be estimated. We henceforth refer to the algorithm developed above as the 'convolved-orthogonal basis reconstruction algorithm' (COBRA).

IV. Algorithm Evaluation

The algorithm is first applied to a single slice of a dynamic realistic mathematical cardiac torso (MCAT) phantom [9], and then to a ^{99}Tc-teboroxime myocardial patient study.

A. Phantom study

The 3D MCAT phantom is shown in Figure 1. This phantom models not only the myocardium, but also the myocardial blood pool, the background activity in the body, and the liver. The projections of a single slice transverse to the long axis of the body were chosen for this evaluation.

The simulated dataset was acquired over 15 rotations of a single-headed camera, taking 120 regularly spaced angular measurements per rotation, of 64 projection bins each. The total imaging period was 15 minutes. While attenuation was modeled, non-ideal system response and scatter were not.

A total of 6 regions, having the TAC's illustrated in Figure 4, were included in the phantom data.

The orthogonal basis functions were calculated through the application of the SVD to a matrix of 100 sampled exponential functions parameterized by rate constants logarithmically spaced in the interval $[5 \times 10^{-4}, 2]$. This interval includes the true range of $k_{12} \in [0.002, .6]$ from which the TAC's are derived. In practice, of course, the true range is unknown, so the choice of interval for k_{12} should ensure that all physiologically feasible modes are accommodated. The number M of left singular vectors $\mathbf{u}_m$ retained after application

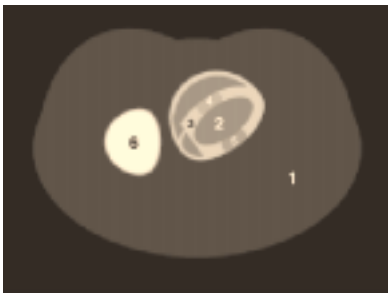

Figure 1: 3D MCAT emission phantom, of which a single slice through the myocardium transverse to the long axis of the body is taken as 2D phantom for these studies. The liver (region 6) is shown to the left of the heart in this illustration. We see that the myocardium contains two defects (darker regions 4 and 5) and normal region 3, which is rendered non-contiguous by the defects. Region 2 is the myocardial blood pool, while region 1, represents the background activity in the torso.

of the SVD is selected as the minimum number needed to approximate all of the exponential functions $f_m[l]$ to within 1% peak deviation, using the reduced-dimension basis. An additional basis function $u_{M+1}[l] = \delta[l]$ is included to allow for explicit modeling of the blood pool within the imaged distribution, where $\delta[l]$ is the discrete-time impulse. The basis functions employed appear in Figure 2

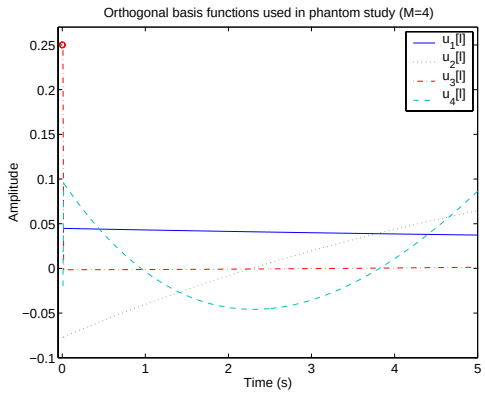

Figure 2: Orthogonal basis functions employed in phantom study. These are the first 4 left singular vectors $\mathbf{u}_m$ of $\mathbf{U}$.

The algorithm was tested over $I = 100$ and $I = 1000$ sinogram realizations. The mean of all estimates $\hat{\boldsymbol{\mu}}_i$ was compared to the true $\boldsymbol{\mu}$ (as recovered from noise-free projection data) to evaluate bias in the estimates. Owing to the parameter redundancy inherent in functions involving exponential sums, we do not attempt to recover this form of parameterization for the recovered TAC's. Rather, we use the following metric to express the deviation between the recovered $\hat{f}_n[l]$ and the true TAC's:

$$M_{\text{dev}} \triangleq \frac{1}{N}\sum_{n=1}^{N} \frac{\sqrt{\frac{1}{L}\sum_{l=1}^{L}\left(f_n[l]-\hat{f}_n[l]\right)^2}}{\max_{l\in\{0,1,\cdots,L-1\}}\left(f_n[l]\right)} \times 100. \qquad (12)$$

For those parameters which are found to be unbiased, the variance of each estimate is subsequently compared to its Cramér-Rao lower bound. When the contribution of a specific basis function towards a TAC is negligible, even negligible estimation errors produce large parameter biases. Consequently, it is appropriate to perform analysis of parameter bias and variance only on those coefficients which are large enough so as to introduce significant power into the recovered TAC. To this end, we introduce the metric:

$$M_{\text{pow}}^{mn} = \frac{\left\|\mu_{mn}\mathbf{c}_m\right\|^2}{\left\|\sum_{m=1}^{M}\mu_{mn}\mathbf{c}_m\right\|^2} \times 100, \qquad (13)$$

where $\mathbf{c}_m$ is the mth convolved basis function and $\|\cdot\|$ denotes the Euclidean norm.

B. *Patient study*

To establish whether the COBRA algorithm is able to produce useful estimates of regional TAC's in a clinical setting, we apply the algorithm to a single transverse slice from a ^{99}Tc-teboroxime myocardial patient study. While the true regional kinetics for this dataset are unknown, we are able to compare our results with those obtained previously through application to the same data of the methods of Formiconi [10] and the direct single compartment fit to projection data (DSCFP) algorithm of Reutter et al. [2].

The method of data acquisition is described in [2]. Briefly, a three detector SPECT study was conducted, having a duration of 15 minutes, during which a full (360°) set of 120 angular projections was acquired every 10 s. An attenuation map was constructed using a transmission source, to allow for attenuation compensation.

The imaged distribution was delineated into the regions: left ventricular myocardium, blood pool, liver and background tissue using the automated volume of interest specification algorithm described in [2]. The 2D slice illustrated in Figure 3 was selected for the purpose of algorithm evaluation.

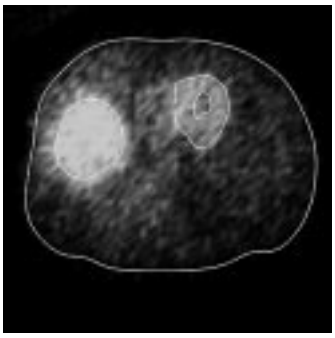

Figure 3: Specific 2D slice through imaged torso, the projections of which are selected for algorithm evaluation. The contours shown delineate tissue regions.

One of the primary motivations for the development of algorithms able to reconstruct imaged distributions directly from projections is the ability of such algorithms to base estimates on projection data which are temporally inconsistent. In order to artificially introduce projection inconsistency,

we significantly decrease the time resolution of the study by summing each set of 4 sequentially acquired sinograms. This yields a set of 22 sinograms sampled at 40 s intervals. Since the activity of regions within the distribution changes by more than 100% during intervals of this length, a large degree of inconsistency is present in this reduced data set.

V. Experimental results

A. Phantom study

Figure 4 compares the original regional TAC's and the mean TAC's recovered by the COBRA algorithm at a total sinogram count value of 2.5×10^5.

Note that we have only processed data from the first 5 camera rotations, as inclusion of the data obtained during the final 10 revolutions did not materially affect the estimates obtained. This behaviour stems from the highly overdetermined nature of the linear system solved by the algorithm.

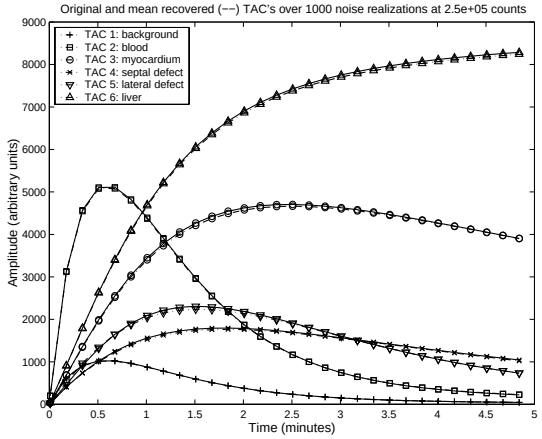

Figure 4: At 2.5×10^5 counts, the mean TAC's recovered over 1000 noise realizations (–) fit the true (phantom) data closely.

Table 1 contains the results of three tests, each of 100 noise realizations at respective count totals per slice of $5 \times 10^5, 2.5 \times 10^5$ and 1×10^5.

Test	Counts	Flops	RMS error ($M_{\text{dev}}\%$)					
			TAC 1	TAC 2	TAC 3	TAC 4	TAC 5	TAC 6
1	5.0e+05	1.1e+08	0.18	0.58	0.75	6.98	4.35	0.27
2	2.5e+05	1.1e+08	0.17	0.87	1.11	8.88	5.58	0.51
3	1.0e+05	1.1e+08	0.19	1.09	1.54	14.69	8.44	0.46

Table 1
Results of 100 noise realization tests of the parameter estimation algorithm.

Most of the errors were well below 5%, even at the lowest total counts value of 10^5 tested. TAC 4, which contains the least power of all the TAC's is also the most poorly recovered, with a worst case error of $M_{\text{dev}} = 14.7\%$.

We see from Table 2, that absolute bias is below 1% for all parameters for which M_{pow} is above 4%. Parameter 4 of TAC 4 (μ_{44}) is the most poorly estimated of all parameters, with a bias of 124%. The convolved basis function scaled by this parameter contains less than 0.1% of the total power within TAC 4, so this bias is not a significant source of error.

	TAC 1	TAC 2	TAC 3	TAC 4	TAC 5	TAC 6
% power in subTAC 1	42.3	42.2	95.2	86.0	73.4	104.1
% bias in coefficient 1	−0.24	−0.35	−0.61	−1.74	−1.40	−0.57
Var. as % of CRLB.	115.56	118.05	113.46	120.49	107.59	117.03
% power in subTAC 2	55.6	55.7	2.7	10.7	21.5	0.0
% bias in coefficient 2	−0.66	−0.52	−2.66	−0.54	−0.77	−2.64
Var. as % of CRLB.	115.30	112.37		123.88	118.42	
% power in subTAC 3	77.9	77.4	0.7	2.5	3.0	0.4
% bias in coefficient 3	−0.48	−0.77	0.13	0.67	10.73	−0.98
Var. as % of CRLB.	114.05	120.49	111.52	132.11		120.37
% power in subTAC 4	2.6	2.5	0.0	0.0	0.1	0.0
% bias in coefficient 4	−0.21	−1.24	12.54	124.32	−40.58	−5.26
Var. as % of CRLB.	114.51	130.09				

Table 2
Quantities used in analysis of parameter bias and variance. These statistics were obtained over 1000 noise realizations, using a set of 4 basis functions $\mathbf{u}_m$ which were all mutually orthogonal before convolution with the blood input function. The 1000 measured sinograms contained 2.5×10^5 counts each over 15 revolutions. Only the first 5 revolutions were used to produce these results. The Cramér-Rao lower bound is abbreviated as 'CRLB'.

We see also from Table 2 that variances for the estimates for those coefficients which significantly weight the TAC's are reasonably close to the Cramér-Rao lower bound, and do not exceed it by more than 30%. Analysis of parameter variance is performed only for those parameters exhibiting less than 2% absolute bias. The COBRA algorithm executes in under 15 s on a Pentium II 450 MHz processor for the tests presented here.

B. Patient study

Figure 5 compares TAC's derived by applying Formiconi's method to those obtained using the COBRA algorithm presented here. Corresponding TAC's appear similar, and the decreased time resolution and greater smoothness of the COBRA TAC's is evident. Quantitatively, we have $M_{\text{dev}} = 9.4\%$.

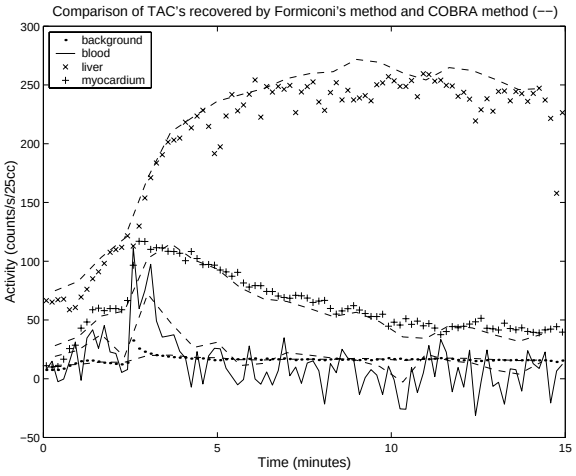

Figure 5: Comparison of TAC's recovered via Formiconi's method and using the reduced-dimension basis estimator (dashed lines).

In Figure 6, TAC's derived through application of the DSCFP due to Reutter et al. are compared to the COBRA TAC's. Since the latter method was applied towards the estimation of myocardial and liver activities alone, while Formiconi's method was employed to determine the

background and blood pool TAC's, only the two former responses are shown. Again, the two sets of curves compare favorably, with $M_{\text{dev}} = 7.3\%$.

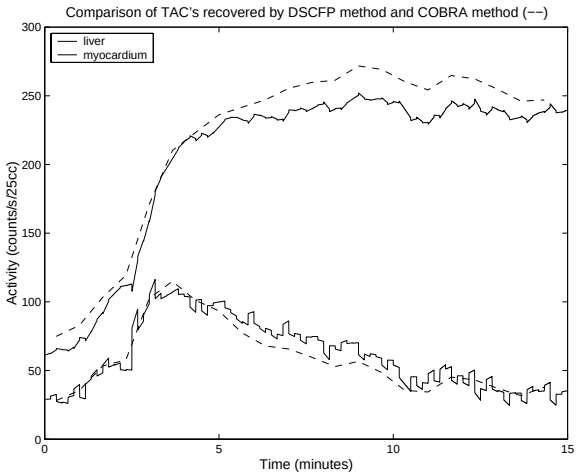

Figure 6: Comparison of TAC's recovered via the direct fit of a single compartment model to projection data (method of Reutter et al.) and the COBRA method. Blood and background TAC's are not shown, as Formiconi's method was used to estimate these in [2]

VI. Discussion

The experimental results indicate that the COBRA algorithm proposed is able to rapidly recover TAC's from temporally inconsistent dynamic SPECT datasets. In phantom studies, the recovered parameters typically exhibit a small bias of the order of 3%, and estimator efficiency is within 30% of the Cramér-Rao lower bound on parameter variance. When applied to a clinical myocardial SPECT study rendered temporally inconsistent through artificial reduction of time-resolution, the recovered curves compared favorably with those obtained through application of the methods of Formiconi and Reutter et al. to high temporal resolution data.

While many previous algorithms have required access to powerful computing equipment when applied to large multislice, multiregion studies, we have demonstrated an algorithm which scales approximately as $O(RPQ(MN)^2 + (MN)^3)$ with $M \approx 4$ rather than $M \approx 100$ as in the spectral method of Cunningham et al. The method of Reutter et al. is more complex, scaling approximately as $O(RPQN^4 + N^5 + N^3)$ per iteration. However, for typical large clinical datasets with few regions (RPQ large), computation is dominated by the $O(RPQN^4)$ term and the DSCFP and COBRA algorithms incur similar computational cost for $M \approx N$. The computation time required for the application of COBRA to the clinical study using a personal computer was 35 s versus 58 s for the DSCFP algorithm.

VII. Acknowledgments

We thank Dr. GT Gullberg and Dr. EVR Di Bella of the Department of Radiology at the University of Utah for providing the patient data, and the Medical Imaging Research Laboratory at the University of North Carolina for making the MCAT phantom available for our simulation studies.

This work was supported in part by the National Heart, Lung, and Blood Institute of the U.S. Department of Health and Human Services under grants HL-07367, R01-HL50663 and P01-HL25840; in part by the Director, Office of Science, Office of Biological and Environmental Research, Medical Sciences Division of the U.S. Department of Energy under contract DE-AC03-76SF00098; and in part by the South African National Research Foundation.

VIII. References

[1] B. W. Reutter, G. T. Gullberg, and R. H. Huesman, "Kinetic parameter estimation from attenuated SPECT projection measurements," *IEEE Transactions on Nuclear Science*, vol. 45, no. 6, pp. 3007–3013, 1998.

[2] B. W. Reutter, G. T. Gullberg, and R. H. Huesman, "Kinetic parameter estimation from dynamic cardiac patient SPECT projection measurements," in *1998 IEEE Nuclear Science Symposium and Medical Imaging Conference Record*, pp. 1953–1958, 1999.

[3] V. J. Cunningham and T. Jones, "Spectral analysis of dynamic PET studies," *Journal of Cerebral Blood Flow and Metabolism*, vol. 13, pp. 15–23, 1993.

[4] P. Chiao, J. A. Fessler, K. R. Zasadny, and R. L. Wahl, "Spectral analysis using regularized non-negative least-squares estimation," in *IEEE Nuclear Science Symposium and Medical Imaging Conference*, vol. 3, pp. 1680–1683, Oct. 1995.

[5] J. S. Maltz, E. Polak, and T. F. Budinger, "Multistart optimization algorithm for joint spatial and kinetic parameter estimation from dynamic ECT projection data," *IEEE Transactions on Medical Imaging, in review.*, 1999.

[6] C. Lanczos, *Applied analysis*. Prentice-Hall, 1956.

[7] J. G. Reich, "On parameter redundancy in curve fitting of kinetic data," in *Kinetic data analysis : design and analysis of enzyme and pharmacokinetic experiments* (L. Endrenyi, ed.), ch. IV, pp. 39–60, Plenum Press, 1981.

[8] F. O'Sullivan, "Imaging radiotracer model parameters in PET: A mixture analysis approach," *IEEE Tranactions on Medical Imaging*, vol. 12, pp. 399–411, Sept. 1993.

[9] B. M. W. Tsui, J. A. Terry, and G. T. Gullberg, "Evaluation of cardiac cone-beam single photon emission computed tomography using observer performance experiments and receiver operating characteristic analysis," *Investigative Radiology*, vol. 28, no. 12, pp. 1101–12, 1993.

[10] A. R. Formiconi, "Least squares algorithm for region-of-interest evaluation in emission tomography," *IEEE Transactions on Medical Imaging*, vol. 12, no. 1, pp. 90–100, 1993.